Journal of Systems Engineering and Electronics
Vol. 28, No. 6, December 2017, pp.1072 – 1077

Radar cross section of arbitrary polished spheres at terahertz frequencies

Ruijun Wang[1,2], Bin Deng[1,*], Hongqiang Wang[1], and Yuliang Qin[1]

1. College of Electronic Science and Engineering, National University of Defense Technology, Changsha 410073, China;
2. Uint 95876 of PLA, Zhangye 734100, China

Abstract: We develop an efficient method for polished metallic sphere's scattering prediction in terahertz band when its frequency dispersion property is considered. By deducing scattering solution of the lossy metallic sphere, the radar cross section (RCS) of different metallic spheres is given at terahertz frequencies. The investigation of the RCS of polished metallic spheres shows the normalized RCS is always same to the metals' normal incidence reflectivity when the sphere becomes electrically large. The metals which have high reflectivity (such as Al, Cu, Ag and Au) show that the corresponding RCS of the spheres is almost πa^2 in terahertz band. The sphere's RCS of the transition metal such as Fe begins to decrease obviously since the far infrared.

Keywords: terahertz, radar cross section (RCS), sphere, Drude model, frequency dispersion.

DOI: 10.21629/JSEE.2017.06.05

1. Introduction

There is increasing interest in studying of the target's scattering characteristics in terahertz band [1 – 3]. The study of the interaction between the metallic targets and the terahertz wave is urgent and necessary for both the terahertz civil and military applications [4,5].

In microwave band, the constant value of conductivity describes metals well because the displacement currents are much smaller than the conduction currents. This is the underlying reason that the metallic targets are often computed with the assumption of perfectly electrical conducting (PEC). However, metallic conductors start changing their properties in upper-millimeter-wave band and above, the assumption of direct current (DC) conductance is not accurate any longer. A new model should be proposed for explaining metals' characterization [6,7]. Naturally, the terahertz scattering characteristic of metals is different from that at microwave frequencies.

In the past, the optical properties of metals had been universally studied. The Drude model and the Drude-Lorentz model have made a great success in depicting metals' property in the optical frequencies and the infrared respectively [8,9]. The optical constants of different metals can be found in [10]. Meantime, several research teams in the world had found discrepancies between the theoretical model prediction and loss measurements for metals at sub-millimeter-wave frequencies [11,12]. Related papers had investigated the normal metals' published experimental data of surface resistance from the frequency of DC up to the mid-infrared [13]. The investigation in [13] shows that the Drude's model is successful for depicting normal metals in DC to the mid-infrared frequency. With the development of terahertz time domain spectroscopy system, the properties of metals in terahertz band were also studied recently. The measurement data were also compared with the Drude model and discussed with the Kramers-Kronig analysis [14 – 16]. From metals' frequency dispersion models of complex permittivity, the terahertz scattering characteristic of metallic targets can be studied exactly.

Electromagnetic scattering from spheres had been studied universally because of its inherent symmetry and its agreement in shape with many natural objects. The researchers in radar community treat the metallic sphere as a reference for radar cross section (RCS) measurement because the metallic sphere is symmetrical and its RCS value is known [2,17]. In terahertz band, the metallic sphere's accurate RCS should be evaluated renewedly because of the frequency dispersion of metals. The modern formulation of the scattering from spheres was given by Gustav Mie in 1908 using the separation of variables, along with the boundary conditions [18]. However, the scattered field formulation diverges for lossy medium because of Riccati-Bessel functions and their derivative in the formulation. In terahertz band, metals have large imaginary parts of the complex permittivity and the scattered field formulation cannot give exact results. Therefore, the direct solving to

Manuscript received October 21, 2015.
*Corresponding author.
This work was supported by the National Science Fund for Young Scientists of China (61302148; 61571011).

scattered field coefficients with the complex dielectric permittivity of metals is improper. Meantime, there is little literature about the analytical solution of a metallic sphere in terahertz band while it is very important for the scattering prediction of targets in the terahertz radar community.

In this paper, the influence of the metal's dispersion on the metallic sphere's RCS is mainly discussed. The accurate monostatic and bistatic RCS of different metallic spheres versus frequencies are computed. The normalized RCS is compared with the normal incidence reflectivity of metals. In the second part of this paper, the theory characterizing the metal's properties and the scattering solution of the lossy metallic sphere are given. In the third part, the RCS for different metallic spheres and the discussions of the numerical results are presented.

2. Theory methods

2.1 Properties of metals in terahertz band

Metals can be characterized with a relatively complex permittivity and a relative complex permeability. The electromagnetic response of a metallic target is decided by the electrons movement within the metals. In the classical Drude model [19], metals are considered as free electron gas. The Drude model gives metals' equivalent relative permittivity as

$$\varepsilon_r = 1 - \frac{\omega_p^2}{\omega^2 - \mathrm{j}\omega\gamma} \tag{1}$$

where ω_p represents the plasma frequency and the damping term γ represents the electron collision rate, which is just the inverse of the mean electron collision time τ, i.e. $\gamma = 1/\tau$. The equivalent complex conductivity can be written as

$$\sigma = \frac{\sigma_0}{1 + \mathrm{j}\omega\tau} \tag{2}$$

where σ_0 is the bulk conductivity at direct current which is independent of the frequency. It can be seen that when $\omega\tau << 1$, thus (2) becomes

$$\sigma = \sigma_0. \tag{3}$$

In practice, the collision time τ in (2) is about tens of femtoseconds. Thus in microwave band, the term $\omega\tau$ is less than one enough. The Drude model will keep consistent with the skin-effect model. It explains the applicability of the relaxation-effect model in microwave band.

For the Drude model, the estimation of the damping frequency and the plasma frequency can be realized through the experimental measurements. The researcher in [20] found that the measured optical constants of metals can be reasonably fit using the Drude model in the infrared and far infrared [20]. Further, the metals' optical properties at sub-millimeter wavelengths had also been measured in [21,22]. The complex permittivity and complex refractive index were obtained from the measured averaged absorptance spectra combined with previous measurements by others. Besides, several groups also measured the metals' reflectivity data in terahertz band [23,24]. It is shown that the measured reflectivity of metals is in agreement with theoretical values computed by the Drude model. Thus, the Drude model is an efficient approximation for characterizing metals in terahertz band and is used in this paper for the analysis of metallic sphere's scattering. In terahertz and the infrared band, some measurements data which verified the accuracy of the Drude model can also be found in [14,16,20]. For different metals, the relative complex permittivity below mid-infrared frequency is given by the Drude model and the related parameters are all shown in Table 1 [20–22]. Above the range of mid-infrared frequency, the relative complex permittivity of metals can be found in [10].

Table 1 Fitted plasma frequency and damping frequency for different metals

Parameter	Metal type				
	Cu	Al	Ag	Au	Fe
ω_p/cm^{-1}	278	660	145	300	156
γ/cm^{-1}	63 800	119 000	72 500	72 500	29 500

2.2 Analytical solution of the lossy metallic sphere

From the above discussion, the boundary conditions of metallic spheres in terahertz band cannot be processed with the assumption of the ideal short circuit boundary because of the finite conductivity. Then we think of the metallic sphere as a lossy dielectric sphere, and the scattered solution can be given in the form of Mie's series. The coefficients of the scattered electrical field are decided by the continuous boundary conditions [25], and can be written as

$$a_n = \frac{\sqrt{\varepsilon_r\mu_r}\hat{J}_n(k_d a)\hat{J}_n'(ka) - \hat{J}_n(ka)\hat{J}_n'(k_d a)}{\sqrt{\varepsilon_r\mu_r}\hat{J}_n(k_d a)\hat{H}_n^{(1)\prime}(ka) - \hat{H}_n^{(1)}(ka)\hat{J}_n'(k_d a)} \tag{4}$$

$$b_n = \frac{\hat{J}_n(k_d a)\hat{J}_n'(ka) - \sqrt{\varepsilon_r\mu_r}\hat{J}_n(ka)\hat{J}_n'(k_d a)}{\hat{J}_n(k_d a)\hat{H}_n^{(1)\prime}(ka) - \sqrt{\varepsilon_r\mu_r}\hat{H}_n^{(1)}(ka)\hat{J}_n'(k_d a)} \tag{5}$$

where a, ε_r and μ_r represent the radius, complex permittivity and complex permeability of the sphere respectively. $k = \omega\sqrt{\mu_0\varepsilon_0}$ is the wavenumber in free space and $k_d = k\sqrt{\mu_r\varepsilon_r}$ is the wavenumber in metal medium. $\hat{J}_n(\cdot)$ is the Riccati-Bessel function of the first kind and the prime means derivative with respect to the argument. $\hat{H}_n^{(1)}(\cdot)$ is the first kind Riccati-Hankel function. The relationship between the Riccati-Bessel functions and the spherical Bessel functions is showed as follows:

$$\frac{1}{ka}\hat{J}_n(ka) = j_n(ka), \quad \frac{1}{ka}\hat{H}_n^{(1)}(ka) = h_n^{(1)}(ka). \tag{6}$$

With (4) and (5), the scattering field of different dielectric spheres can be given accurately. However, for lossy medium such as metals, the Riccati-Bessel functions in (4) and (5) diverge exponentially for linearly increasing $k_d a$, and the rate of divergence would increase with the increasing value of the imaginary part of ε_r. In order to obtain the analytical solution when taking the frequency dispersion of spheres into account, we seek to establish a calculated representation of the scattering coefficients.

Firstly, dividing nominator and denominator of the expression for a_n in (4) by the Riccati-Bessel functions of the first kind $\hat{J}_n(k_d a)$, we get

$$a_n = \frac{\sqrt{\varepsilon_r \mu_r}\hat{J}_n'(ka) - \hat{J}_n(ka)\hat{J}_n'(k_d a)/\hat{J}_n(k_d a)}{\sqrt{\varepsilon_r \mu_r}\hat{H}_n^{(1)\prime}(ka) - \hat{H}_n^{(1)}(ka)\hat{J}_n'(k_d a)/\hat{J}_n(k_d a)} =$$

$$\frac{\sqrt{\varepsilon_r \mu_r}\hat{J}_n'(ka) - \hat{J}_n(ka)D_n(k_d a)}{\sqrt{\varepsilon_r \mu_r}\hat{H}_n^{(1)\prime}(ka) - \hat{H}_n^{(1)}(ka)D_n(k_d a)} \tag{7}$$

where $D_n(k_d a)$ represents the logarithmic derivative of $\hat{J}_n(k_d a)$. The derivatives of the Riccati-Bessel functions can be represented by the spherical Bessel functions as follows:

$$\hat{J}_n'(ka) = kaj_{n-1}(ka) - nj_n(ka) \tag{8}$$

$$\hat{H}_n'(ka) = kah_{n-1}^{(1)}(ka) - nh_n^{(1)}(ka) \tag{9}$$

where $j_n(ka)$ and $h_n^{(1)}(ka)$ are the spherical Bessel functions of order n. According to (6), (8) and (9), the recurrence relations for $D_n(k_d a)$ can be derived as

$$D_{n-1}(k_d a) = \frac{n}{k_d a} - \frac{1}{D_n(k_d a) + n/(k_d a)}. \tag{10}$$

Then, the scattering coefficient can be rewritten as follows:

$$a_n =$$

$$\frac{\sqrt{\varepsilon_r \mu_r}[kaj_{n-1}(ka) - nj_n(ka)] - kaj_n(ka)D_n(k_d a)}{\sqrt{\varepsilon_r \mu_r}[kah_{n-1}^{(1)}(ka) - nh_n^{(1)}(ka)] - kah_n^{(1)}(ka)D_n(k_d a)} =$$

$$\frac{j_{n-1}(ka) - j_n(ka)[n/(ka) + D_n(k_d a)/\sqrt{\varepsilon_r \mu_r}]}{h_{n-1}^{(1)}(ka) - h_n^{(1)}(ka)[n/(ka) + D_n(k_d a)/\sqrt{\varepsilon_r \mu_r}]}. \tag{11}$$

The function $D_n(k_d a)$ keeps finite except for $a \to 0$. Thus a new form of the scattering coefficient which is suitable for computation is obtained. By the downward recurrence, we can calculate the scattering fields of metallic spheres in terahertz band.

Similarly, we can get the same result for b_n.

$$b_n = \frac{j_{n-1}(ka) - j_n(ka)[n/(ka) + \sqrt{\varepsilon_r \mu_r}D_n(k_d a)]}{h_{n-1}^{(1)}(ka) - h_n^{(1)}(ka)[n/(ka) + \sqrt{\varepsilon_r \mu_r}D_n(k_d a)]} \tag{12}$$

In the following, the scattering of typical metallic spheres will be computed in terahertz band and some discussions are also given.

3. Results and discussion

We first take a copper sphere as an example and compute the monostatic and bistatic RCS with the complex permittivity which is given by the Drude model in Table 1 and the experimental data in [20]. We also assume $\mu_r = 1$ for the copper sphere because of its non-magnetism.

Fig. 1 shows the monostatic normalized RCS of a polished copper sphere of 5 mm in radius versus the frequencies. In contrast, the normal incidence reflectivity of the copper is also given. It can be seen that when the frequency is between 10 GHz to 300 GHz, the copper sphere is in the resonance region. The reflectivity is almost unity. At the frequencies above 300 GHz, the sphere enters the optical region and the normalized RCS initially keeps nearly unity and then has an obvious falling in the visible light. Meantime, there is a great agreement between the normalized RCS and the normal reflectivity in the optical region. In fact, the RCS of metallic spheres in the optical region can be expressed as the product of a PEC sphere's RCS and the normal incidence reflectivity of this metal. When the metallic sphere's RCS is normalized with πa^2, the result of RCS will be equal to the normal reflectivity of corresponding metals. Thus it can be seen that the experimental data of normal reflectivity can be used to verify the numerical results [10,20]. The decrease in the normalized RCS is caused by the enhanced absorption and transmission of electromagnetic waves for metals at higher frequencies, i.e. the transparency of metals at ultraviolet.

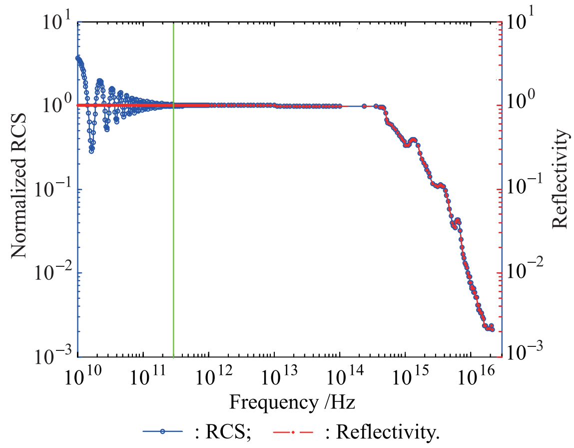

Fig. 1 Comparison result of the normalized RCS [RCS/πa^2] and the normal reflectivity for the copper sphere

Similarly, the other metallic spheres such as Ag, Au, Al and Fe can be investigated. However, the permeability for the transition metal such as Fe should be considered. According to the generalized Maxwell relation [19], the complex refractive index is an equivalent optical constant of metals and it is connected with the complex permittivity and the complex permeability by the relationship $n' = n + \mathrm{i} \cdot k = \sqrt{\varepsilon_r \mu_r}$. k represents the extinction coefficient and n represents the index of refraction. The normal incidence reflectivity is also a function of the complex refractive index by

$$R = \frac{(n-1)^2 + k^2}{(n+1)^2 + k^2}. \tag{13}$$

Then, both the complex refractive index and the normal incidence reflectivity depict the interaction between the electromagnetic wave and the target. Instead of the complex permittivity and the permeability, we can investigate the RCS of an iron sphere by the complex refractive index [10,20,21,26]. Fig. 2 shows the normalized RCS of different spheres of 5 mm in radius versus the frequencies, which is correspondingly versus complex refractive index for their frequency dependence relationship. In contrast, we also plot the normalized RCS of a PEC sphere. The results show that the PEC assumption for metals becomes inaccurate with the increase of the frequencies. However, the perceptible falling of the normalized RCS for Ag, Au, Al and Cu spheres occurs above the infrared frequency although the detail comparison and the experimental data of the normal incidence reflectivity of these metals validate that the slight falling begins in terahertz band [23,24]. For the iron sphere, it can be seen that the obvious decrease in the RCS begins due to the far infrared which is lower than the situation of the copper sphere. This can be understood by the property of the transition metals. The decrease in the normal incidence reflectivity of transition metals begins earlier with the increase of the incident wave frequency.

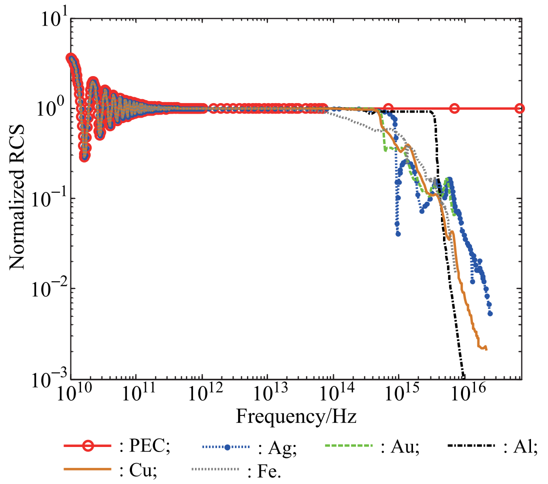

Fig. 2 Normalized RCS [RCS/πa^2] versus frequencies for different metallic spheres

For a polished metallic sphere, the decrease of the normalized RCS can be ascribed to the frequency dispersion of metal medium. According to the Drude model and open access data in [10], the real part and the imaginary part of the complex refractive index for metals are between 0 and 1 000 from microwave to the optical frequencies. In order to understand the decrease of the normalized RCS for metallic spheres, we investigate the effect of the variable complex refractive index on the RCS. Fig. 3 shows the distribution of a sphere's normalized RCS in dB when $ka = 21$. The y-axis denotes the range of the extinction coefficient and the x-axis denotes the range of the index of refraction. Meantime, two tracks of complex refractive index for Al and Fe at different frequencies are plotted. It can be seen that such metals become the dielectric gradually with the increase of frequencies. If a metallic sphere with the RCS of πa^2 has a decrease of 3 dB in amplitude, the normalized RCS becomes 0.501 2 correspondingly. Thus, the normalized RCS which is nearly one means that the polished metallic sphere's RCS is almost πa^2 in terahertz band. On the other hand, we can investigate the sphere's RCS for different media by this distribution image.

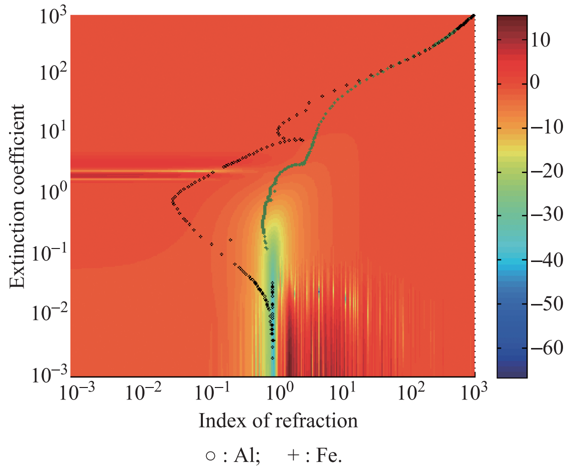

Fig. 3 Distribution of the normalized RCS versus the complex refractive index

The normalized RCS of the electrically large sphere is 0 dB for most media with a large complex refractive index. For lower lossy medium sphere, there is sharp oscillation versus the increasing index of refraction. For medium with an index of refraction of 1 and a small extinction coefficient, the sphere's RCS is lower enough for the full transmission of electromagnetic waves. Thus Fig. 3 supplies a panorama of the sphere's RCS for different materials. From Fig. 3, the normalized RCS for a dielectric ($\varepsilon_r = 3.5 + 0.5\mathrm{i}$) sphere is about -10 dB, which accords with the result of Fig. 2.2.6 in [27]. It also verifies the exactness of the analytical solution above.

The bistatic RCS of a copper sphere of 5 mm in radius is also investigated in Fig. 4. The sphere is an electrically large target when the frequency is above 0.3 THz. The figures for HH and VV polarization are given in the form of semilog plot and the backscattering corresponds to the observation angle of 180° while the forward scattering corresponds to the observation angle of 0°. It can be seen that with the increase of the frequency, the bistatic RCS around the forward observation angle changes obviously. The oscillation range of the bistatic RCS becomes small and the oscillation only exists in a narrower angle around 0°. In addition, the sphere's forward RCS gets larger with the increasing frequency while the backward RCS is almost πa^2 in terahertz band.

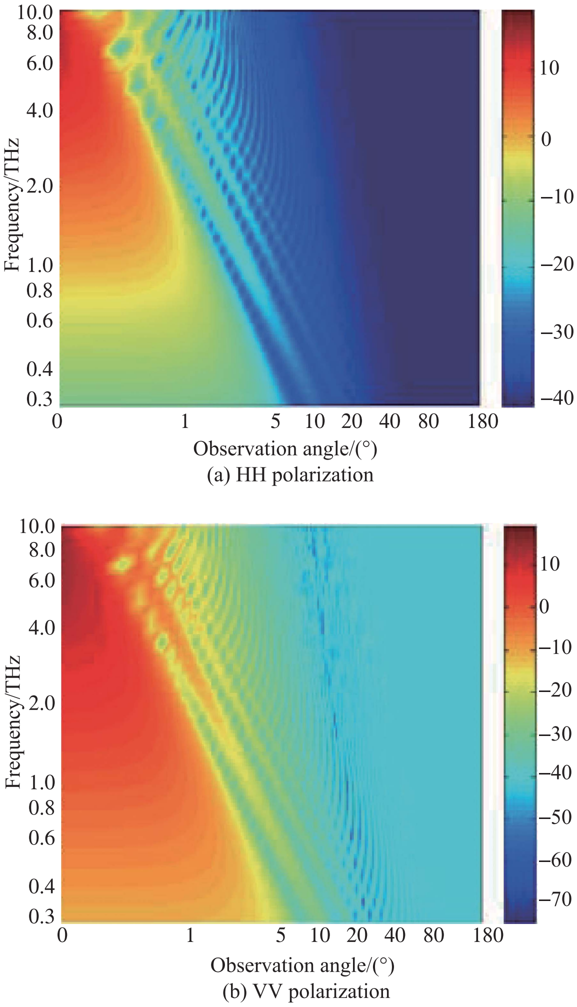

(a) HH polarization

(b) VV polarization

Fig. 4 Bistatic RCS of a copper sphere of 5 mm in radius

4. Conclusions

In summary, the RCS of different metallic spheres in terahertz band is discussed by analyzing the factors of frequency dispersion and analytical solution. The numerical results show that, for an electrically large polished metallic sphere, the monostatic normalized RCS is equal to the normal incidence reflectivity of metals. For metals such as Cu, Al, Au and Ag, their normal incidence reflectivity is closed to one below the frequency of visible light and then the monostatic RCS is almost πa^2. For the transition metal such as iron, the sphere's normalized RCS decreases since the far infrared. Further, the normalized RCS distribution versus the complex refractive index supplies a panorama of the sphere's RCS for different materials, which is helpful for scattering analyzing and understanding of spheres.

References

[1] Z. Li, T. J. Cui, X. J. Zhong, et al. Electromagnetic scattering characteristics of PEC targets in the terahertz regime. *IEEE Antennas and Propagation Magazine*, 2009, 51(1): 39 – 50.

[2] K. Iwaszczuk, H. Heiselberg, P. U. Jepsen. Terahertz radar cross section measurements. *Optics Express*, 2010, 18(25): 26399 – 26408.

[3] H. Y. Li, Q. Li, Z. Xia, et al. Influence of Gaussian beam on terahertz radar cross section of a conducting sphere. *Journal of Infrared, Millimeter, and Terahertz Waves*, 2013, 34(1): 88 – 96.

[4] L. M. Zurk, B. Orlowski, G. Sundberg, et al. Electromagnetic scattering calculations for terahertz sensing. *Proc. of SPIE, Integrated Optoelectronic Devices*, 2007: 64720A.

[5] A. Jagannathan, A. J. Gatesman, T. Horgan, et al. Effect of periodic roughness and surface defects on the terahertz scattering behavior of cylindrical objects. *Proc. of SPIE, Defense Security and Sensing*, 2010: 76710E.

[6] S. Lucyszyn. Comment on "study of excess conduction loss in normal metals at/below sub-millimeter wavelengths" by W. Pan and X. Zhang. *Journal of Infrared, Millimeter, and Terahertz Waves*, 2007, 28(3): 263 – 266.

[7] S. Lucyszyn. Investigation of Wang's model for room-temperature conduction losses in normal metals at terahertz frequencies. *IEEE Trans. on Microwave Theory and Technology*, 2005, 53(4): 1398 – 1403.

[8] J. Lloyd-Hughes, T. Jeon. A review of the terahertz conductivity of bulk and nano-materials. *Journal of Infrared, Millimeter, and Terahertz Waves*, 2012, 33(9): 871 – 925.

[9] M. I. Markovic, A. D. Rakic. Determination of the reflection coefficients of laser light of wavelengths (0.22μm, 200μm) from the surface of aluminum using the Lorentz-Drude model. *Applied Optics*, 1990, 29(24): 3479 – 3483.

[10] D. R. Lide. *CRC handbook of chemistry and physics*. 90th ed. Boca Raton: CRC Press, 2010.

[11] F. J. Tischer. Excess conduction losses at millimeter wavelengths. *IEEE Trans. on Microwave Theory and Technology*, 1976, 24(11): 853 – 858.

[12] R. A. H. R. Schwab. Open resonator studies for the determination of the surface resistance at mm-wave frequencies. *Proc. of the Microwaves and Optronics Conference*, 1997: 106 – 110.

[13] S. Lucyszyn. Investigation of anomalous room temperature conduction losses in normal metals at terahertz frequencies. *IEE Proceedings-Microwaves, Antennas and Propagation*, 2004, 151(4): 321 – 329.

[14] H. Yasuda, I. Hosako. Measurement of terahertz refractive index of metal with terahertz time-domain spectroscopy. *Japanese Journal of Applied Physics*, 2008, 47(3): 1632 – 1634.

[15] D. Zhou, E. P. J. Parrott, D. J. Paul, et al. Determination of complex refractive index of thin metal films from terahertz

time-domain spectroscopy. *Journal of Applied Physics*, 2008, 104(5): 053110.

[16] W. F. Sun, X. Wang, Y. Zhang, et al. Measuring method for refractive index of metal with terahertz time domain reflection spectroscopy. *Proc. of SPIE, Photoelectronic Detection and Imaging*, 2009: 73851F.

[17] R. Gente, C. Jansen, R. Geise, et al. Scaled bistatic radar cross section measurements of aircraft with a fiber-coupled THz time-domain spectrometer. *IEEE Trans. on Terahertz Science and Technology*, 2012, 2(4): 424 – 431.

[18] G. Mie. Beitrage zur optik truber medien, speziell kolloidaler metallosungen. *Annalen der Physik*, 1908, 25(3): 377 – 445.

[19] M. Fox. *Optical properties of solids*. London: Oxford University Press, 2001.

[20] M. A. Ordal, R. J. Bell, R. W. Alexander, et al. Optical properties of fourteen metals in the infrared and far infrared Al, Co, Cu, Au, Fe, Pb, Mo, Ni, Pd, Pt, Ag, Ti, V, and W. *Appied Optics*, 1985, 24(24): 4493 – 4499.

[21] M. A. Ordal, R. J. Bel, R. W. Alexander, et al. Optical properties of Al, Fe, Ti, Ta, W, and Mo at submillimeter wavelengths. *Applied Optics*, 1988, 27(6): 1203 – 1209.

[22] M. A. Ordal, R. J. Bel, R. W. Alexander, et al. Optical properties of Au, Ni, and Pb at submillimeter wavelengths. *Applied Optics*, 1987, 26(4): 744 – 752.

[23] K. L. F. Bane, G. Stupakov, J. J. Tu. Reflectivity measurements for copper and aluminum in the far infrared and the resistive wall impedance in the LCLS undulator. *Proc. of the European Particle Accelerator Conference*, 2006: 2955 – 2957.

[24] P. Tan, Q. Fu, Y. B. Li, et al. Effects of metal mirrors reflectivity and aberrations on the THz FEL radiation performance. *Proc. of International Particle Accelerator Conference*, 2012: 1729 – 1731.

[25] C. F. Bohren, D. R. Huffman. *Absorption and scattering of light by small particles*. New York: Wiley, 2008.

[26] J. H. Weaver, E. Colavita, D. W. Lynch, et al. Low-energy interband absorption in bcc Fe and hcp Co. *Physical Review B*, 1979, 19(8): 3850.

[27] G. Y. He. *Computing and measurement of electromagnetic scattering*. Beijing: Beihang University Press, 2006. (in Chinese)

Biographies

Ruijun Wang was born in 1986. He received his M.S. degree in 2010 and Ph.D. degree in 2015 from National University of Defense Technology (NUDT), China. His research interests include terahertz scattering understanding, and terahertz radar imaging.
E-mail: wandering_jun@163.com

Bin Deng was born in 1981. He received his M.S. degree in 2006 and Ph.D. degree in 2010 from National University of Defense Technology (NUDT), China. He is currently a lecturer in the NUDT. His research interests include terahertz radar imaging, and SAR/GMTI.
E-mail: dengbin@nudt.edu.cn

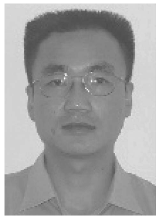

Hongqiang Wang was born in 1970. He received his M.S. degree in 1999 and Ph.D. degree in 2002 from National University of Defense Technology (NUDT), China. He is currently a professor with the College of Electronic Science and Engineering, NUDT. His research interests include radar signal processing, terahertz radar imaging, and automation target recognition.
E-mail: oliverwhq1970@gmail.com

Yuliang Qin was born in 1980. He received his M.S. degree in 2004 and Ph.D. degree in 2008 from National University of Defense Technology (NUDT), China. He is currently an associate professor in NUDT. His research interests include terahertz radar imaging, cognitive radar, and information fusion.
E-mail: qinyuliang@nudt.edu.cn